The stratosphere-troposphere connection in ensemble forecasting

Jan Barkmeijer[*], **Frédéric Vitart**[+], **Martin Leutbecher**[+], **Thomas Jung**[+], **and Jan-Otto Hooghoudt**[*]

[*] *Royal Netherlands Meteorological Institute*
de Bilt, The Netherlands
Jan.Barkmeijer@knmi.nl
[+] *European Centre for Medium-Range Weather Forecasts*
Reading, England

1 Introduction

By now, it has become generally accepted that both the troposphere and the stratosphere play an important role in defining the atmospheric circulation. Baldwin and Dunkerton (1999) showed, by using 40 years of daily data, that the largest amplitude anomalies in the lower stratosphere (around 10 hPa) frequently appear to descend to the troposphere on a timescale of 3 weeks. The predictive skill associated with the downward propagation has been estimated by e.g. Baldwin *et al.* (2003) and Charlton *et al.* (2003), by using statistical models. Both studies conclude that an extra skill of 5% can be obtained in Northern Hemisphere weather on time scales of 10 to 45 days. In fact, already for lead times larger than 5 days, the stratosphere seems to be a better predictor for the tropospheric circulation than the troposphere itself, see e.g., Christiansen (2005) and Siegmund (2005).

In addition to these observational and statistical studies, also a variety of studies have been carried out by using numerical models of the atmosphere. One of the pioneers in this respect was Boville (1984). In order to quantify the impact of inaccuracies in describing stratospheric dynamics, he changed the stratospheric diffusion in his model. He found significant tropospheric changes as compared to his unperturbed run. The response closely resembled the spatial structure of the North Atlantic Oscillation (NAO). In a more recent study Jung and Barkmeijer (2006) employed a version of European Centre for Medium-Range Weather Forecast's (ECMWF) model to investigate the response of model tendency perturbations applied in the stratosphere and especially designed to alter the strength of the stratospheric polar vortex. They found a significant impact on the tropospheric circulation as a result of this extra model forcing. In addition the perturbation growth turned out to be quite linear for realistically sized stratospheric perturbations.

In this paper we will study the impact of analysis perturbations based on stratospheric singular vectors (SV). Since, for example, highly nonlinear boundary layer and precipitation generating processes play no role in the stratosphere (Haynes, 2005), it is very well possible that the linear approximation in the stratosphere is valid for longer forecast times than it is the case for the troposphere. The results in Jung and Barkmeijer (2006) confirm this view. Therefore, we decided to use an optimization time interval of 5 days in the calculation of the stratospheric SV's. The impact of stratospheric analysis perturbations has been studied with the ECMWF monthly forecasting system, which runs operationally since October 2004 (Vitart, 2004). It was found recently (Jung and Leutbecher, 2007) that the observed stratosphere-troposphere link ('downward propagation' of stratospheric anomalies), which may provide a potential source of extended-range predictability in high latitudes, is realistically represented in these monthly integrations. During the period, which we selected to perform ensembles with monthly lead time, a stratospheric sudden warning (SSW) occurred. This is one of the most dramatic stratospheric events and it is associated with a complete breakdown of the stratospheric polar vortex

and a sudden increase in temperature over the polar region. For an overview, see Labitzke (1999).

The structure of the paper is as follows. In the next section a description of stratospheric SVs, together with some of their basic properties, will be given. This is followed by a section on the experimental set-up with the monthly forecasting system and on the results obtained with various ensemble configurations. The paper concludes with the main findings of this study.

2 Stratospheric singular vectors

The defining equation of stratospheric SV's closely follows the one used for tropospheric SV. It reads as:

$$\mathbf{E}^{-1/2}\mathbf{P}_{ini}^{*}\mathbf{M}^{*}\mathbf{P}_{evo}^{*}\mathbf{E}\mathbf{P}_{evo}\mathbf{M}\mathbf{P}_{ini}\mathbf{E}^{-1/2}\mathbf{v}_{i}(0) = \sigma_{i}^{2}\mathbf{v}_{i}(0). \tag{1}$$

Nearly the same eigenvalue problem has to be solved for tropospheric SV's (e.g., Buizza and Palmer, 1995); the difference is the use of projection operator $\mathbf{P_{ini}}$ and $\mathbf{P_{evo}}$ to which we come back later.

The components of the eigenvectors $\mathbf{v}_i$ comprise vorticity, divergence, temperature and logarithm of the surface pressure. The forward propagator $\mathbf{M}$ is the linear operator that describes the linear evolution of perturbations along the nonlinear trajectory during an Optimization Time Interval (OTI), which is set to 5 days in this paper. The projection operators $\mathbf{P_{ini}}$ and $\mathbf{P_{evo}}$ confine the region (horizontally as well as vertically) where a perturbation initially is located ($\mathbf{P_{ini}}$) and where, at final time, perturbation energy is maximized ($\mathbf{P_{evo}}$). We have used the total energy (TE) norm (Errico, 2000) as expressed by $\mathbf{E}$ both at initial and final time and furher $\mathbf{M}^*$, for example, denotes the adjoint of $\mathbf{M}$ with respect to the Euclidean inner product.

The properties of two types of SV's, which we shall consider in this paper, are controlled by defining suitable projection operators $\mathbf{P_{ini}}$ and $\mathbf{P_{evo}}$. We distinguish the following two types of SV's (see also Fig. 1):

- **S-SV**'s (stratospheric SV's) start in the (low) stratosphere (10-100 hPa) and produce maximal total energy perturbation growth in the same vertical zone. Here $\mathbf{P_{ini}}$ and $\mathbf{P_{evo}}$ both set the model state vector to zero outside the 10-100 hPa part of the atmospheric column. In addition $\mathbf{P_{evo}}$ also projects horizontally onto the area north of 30ºN.

- **ST-SV**'s (stratospheric-tropospheric SV's) also start in the low stratosphere (10-100 hPa) but produce maximal perturbation total energy in the low troposphere (500-1000 hPa). Here $\mathbf{P_{ini}}$ and $\mathbf{P_{evo}}$ set the state vector to zero outside the vertical zone (10-100 hPa) and (500-1000 hPa) respectively. Again $\mathbf{P_{evo}}$ projects horizontally onto the area north of 30ºN.

In the following sections we briefly discuss some basic properties for both types of stratospheric SVs. More details can be found in Hooghoudt and Barkmeijer (2007). The horizontal resolution of the SV computation was set to a triangular truncation at wavenumber 42 and a recent version of the ECMWF model (32R2) was used, together with the corresponding adiabatic linear models. For the vertical resolution we have used 62 and 91 levels. Compared to the 91 level model, the vertical resolution of the 62 level model is coarser above 150 hPa, with 15 instead of 45 levels and with the model top extending to 5 hpa instead of 0.01 hPa. Here we shall focus on the 91 level results. Earlier S-SV computations have been performed by Hartmann *et al.* (1996) with only three model levels in the stratosphere.
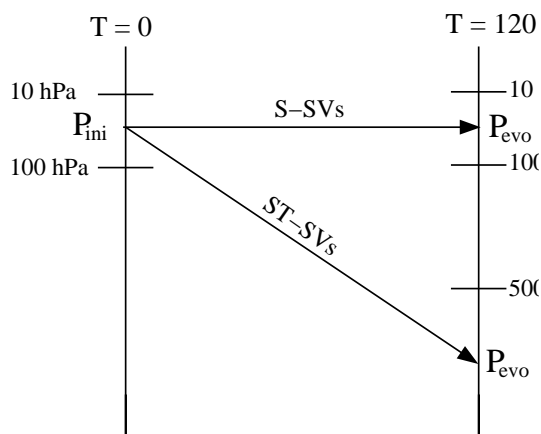
Figure 1: Schematic representation of the two SV configurations. $\mathbf{P_{ini}}$ *and* $\mathbf{P_{evo}}$ *refer to the projection operators used at initial and final time respectively.*

2.1 Amplification

Figure 2 shows the amplification of S-SVs and ST-SVs during January 2006 for an optimization time of 2 and 5 days. Clearly the amplification of stratospheric SV's is smaller than their tropospheric counterparts and ST-SV's amplify less than S-SV's. In particular the results reveal that 2 days are too short for stratospheric perturbations to amplify in the troposphere. The ST-SVs results with an optimization time of 5 days show quite intermittent behaviour with larger amplification during 11-14 January and towards the end January. During both periods the singular values of tropospheric SVs (with 2 and 5 days optimization time) appear to be larger as well. For S-SVs, the SSW and the period of its decaying phase (20-31 January) results in larger amplification.

2.2 Energy profiles

In contrast to the generally accepted point of view that wavenumber 1-3 should be dominant in vertically propagating perturbations (e.g., Charney and Drazin, 1961), it was found that higher wavenumbers were more important in transferring energy. Moreover, forcing ST-SVs to be large scale by setting the contribution of total wavenumber larger than 3 to zero in the SV computation, also resulted in amplifying vertically perturbations in winter as well as in summer. Figure 3 shows the total energy per total wavenumber of the leading SV during January 2006 at initial time (dashed) and of the component of the time evolved SV that enters the troposphere below 500 hPa. At initial time the ST-SV's appear to be larger scale than S-SV's. In fact, S-SVs share many properties with tropospheric SV's, such as, up-scale perturbation growth. The energy profiles below 500 hPa are quite similar for both types of SV's and their shape hardly changes with increasing lead time.
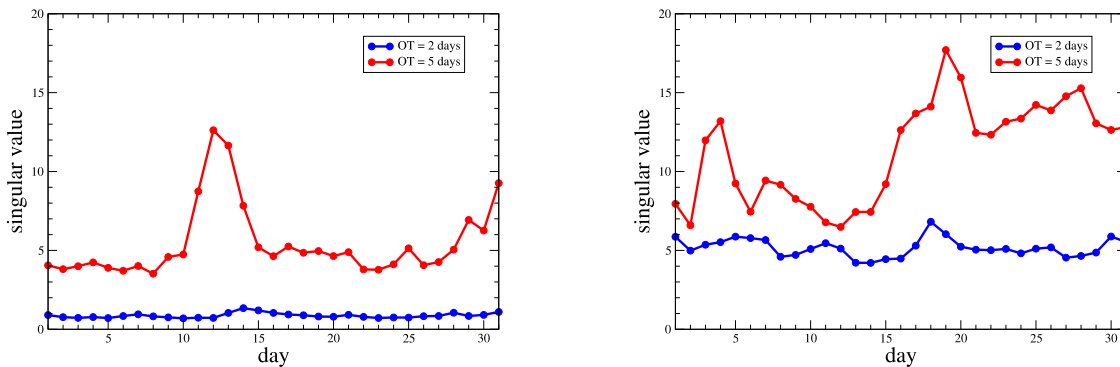
Figure 2: Left panel: singular value of the leading daily ST-SV during January 2006 with an optimization time of 2 (blue) and 5 days (red); Right panel: same but for S-SV's.
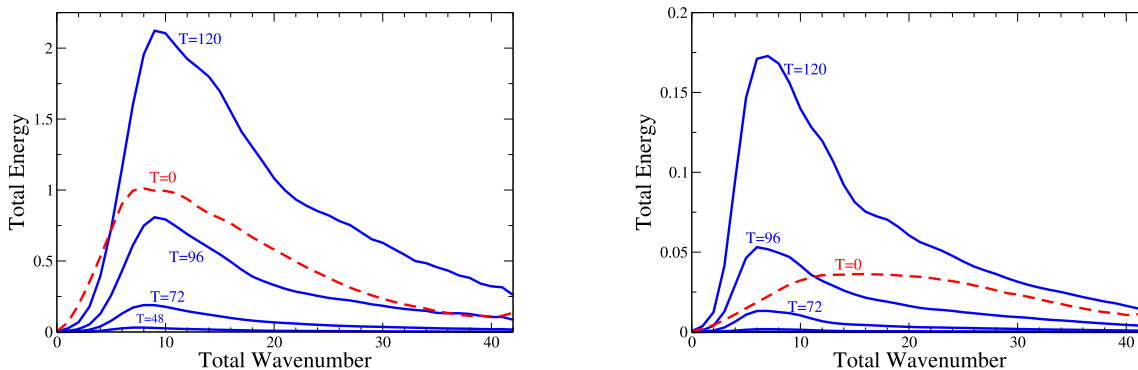

Figure 3: Energy profiles for ST-SV's (left panel) and S-SV's (right panel). The initial time profiles are given by dashed lines; the solid lines indicate energy profiles below 500 hPa of the linearly evolved leading SV for various lead times.

3   Experimental set-up

To examine the impact of stratospheric initial condition perturbations in an ensemble system, a nine week period was selected: 22 December 2005 to 23 February 2006. The ECMWF monthly forecasting system (Vitart, 2004) with a recent model version (32R2) was run every week, starting with 22 December 2005. Note that during the nine week period a well observed SSW took place, which led to a considerable warming during 23-27 January 2006. Every ensemble run with the monthly forecasting system comprises 50 members at a $T_L 159$ horizontal resolution. They differ in their vertical resolution or in the type of perturbations (with respect to initial condition and model) that is applied. Table 1 gives an overview of the various ensemble configurations.

TABLE 1. LIST OF ENSEMBLE CONFIGURATIONS

62 levels	operational setting
	operational setting, and with S-SVs
91 levels	operational setting
	operational setting, and with S-SVs
	only S-SVs
	only ST-SVs
	only S-SVs, and no stochastic physics
	only ST-SVs, and no stochastic physics

4   Results

4.1   impact of vertical resolution

Increasing the vertical resolution from 62 to 91 levels, which affects the model resolution above 150 hPa, leads to an improvement of the performance of the monthly forecasting system mainly in the stratosphere (see also section 4.3). As an example of how the L62 and L91 ensembles compare for the operational setting, we show in Fig. 4 the plume for 19 January 2006 in terms of the temperature gradient at 50 hPa (ΔT50) between polar cap (80ºN-90ºN) and mid-latitudes (50ºN-60ºN). Positive values are indicative for an occurence of a SSW. Already during the initial phase of the forecast the L62 ensemble temperature gradients differ considerably from the analysed gradient as given by the black solid line. The L91 ensemble captures much better the magniude of SSW. The improved stratospheric performance for the L91 ensemble is also noticeble from the ensemble mean in terms ΔT50, see Fig. 4. The standard deviation for ΔT50, which partly results from tropospheric perturbations, is nearly similar for both settings of the vertical resolution (similar conclusion holds for other variables, not shown).
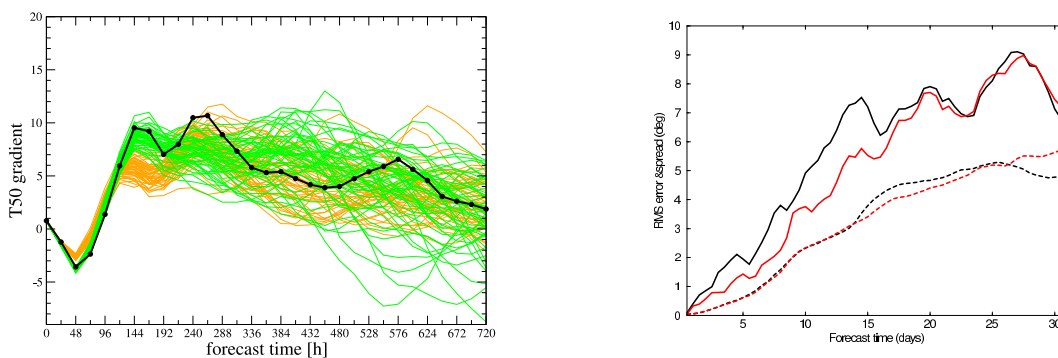

Figure 4: Left panel: plume for the meridional temperature gradient ΔT50 (see text for more details) for the ensemble with operational setting starting on 19 January 2006 with 62 levels (orange) and 91 levels (green), and the observed gradient (black solid line); Right panel: the ensemble mean error and ensemble standard deviation in terms of ΔT50 (solid and dashed line respectively) for the L62 (red) and L91 (black) ensembles.

4.2 impact of stratospheric perturbations

Stratospheric perturbations, derived from S-SVs or ST-SVs by Gaussian sampling, lead to a considerable increase in ensemble spread, particularly in the stratosphere. Figure 5 shows the ensemble standard deviation for $\Delta T50$ in case of the two L62 configurations (see Table 1). Clearly, the impact of S-SVs is noticeble up to day 15. The $\Delta T50$ plume for 19 January 2006 produced by the L91 ensemble with operational setting and using S-SVs (see Fig 5) is much broader now. Note that all members indicate the occurence of a SSW though.
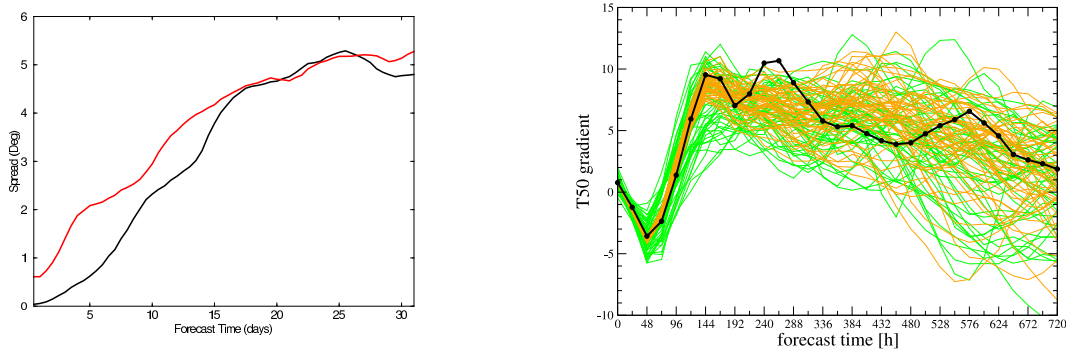

Figure 5: Left panel: L62 ensemble standard deviation in terms of $\Delta T50$ for the configuration with operational setting (black) and with S-SV's added (red); Right panel: $\Delta T50$ plume for the L91 ensemble starting on 19 January 2006 with operational setting (orange) and with S-SV's added (green), and the analysed gradient (black solid line).
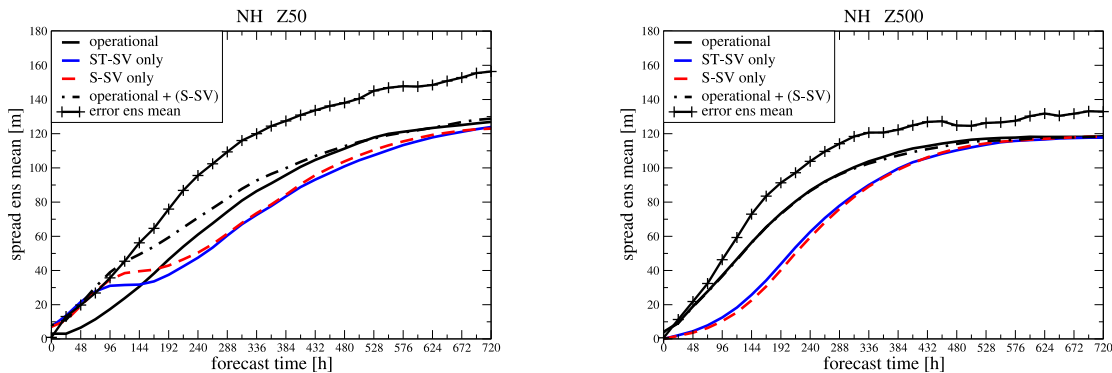

Figure 6: Left panel: standard deviation in terms of Z50 for the operational ensemble configuration (solid black), ST-SV's only (solid blue), S-SV's only (dashed red) and operational with S-SV's (chain dashed) end error of operational ensemble mean (+) ; Right panel: same but for Z500.

The impact of stratospheric perturbations on the troposphere, however, remains small when combined with tropospheric perturbations, as can be inferred from Fig. 6 (right panel: solid and chain dashed line). For this reason we ran additional L91 ensembles to isolate more the impact of stratospheric perturbations onto the stratosphere and troposphere. Figure 6 shows the ensemble standard deviation in terms of geopotential height at 50 hPa (Z50) and 500 hPa (Z500) when only analysis perturbations based on S-SV's or ST-SV's are used. The

Z50 ensemble standard deviation behaves as one would expect from the SV amplification: the ST-SV ensemble has smaller spread than the S-SV ensemble at optimization time (120 hours). See also Fig. 7, where the spatial pattern of the Z50 standard deviation is plotted for four ensemble configurations. Surprisingly the standard deviation initially keeps pace with the root mean square (RMS) error of the ensemble mean, but stagnates around the optimization time. For longer forecast times, the two ensemble configurations using tropospheric perturbations even take the lead in producing spread. Yet all ensemble configurations yield considerably less spread than the RMS error of the ensemble mean.
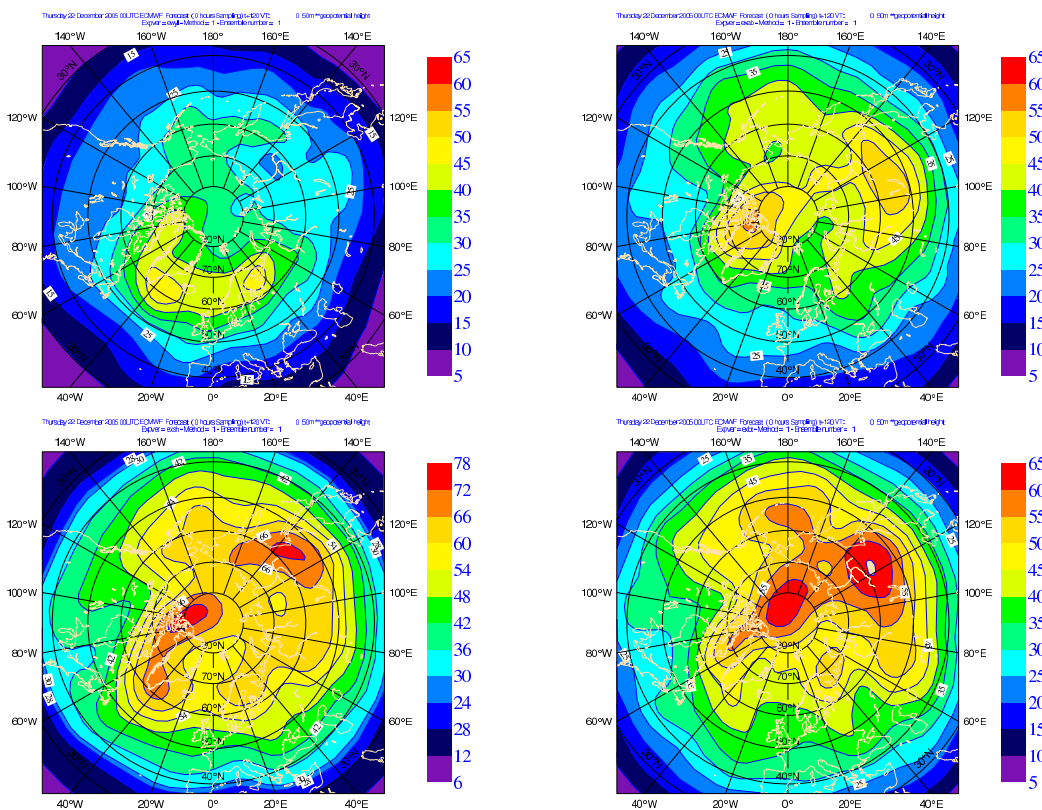

Figure 7: Standard deviation for Z50 at t=120 hours for ensembles with operational setting (top left), with S-SV's added (bottom left), with ST-SV's only (top right) and with S-SV's only (bottom right).

The Z500 results for the S-SV and ST-SV only ensembles make clear that stratospheric perturbations are very well capable to produce ensemble spread in troposphere. As anticipated, the S-SV based configuration has smaller standard deviation than the ST-SV based configuration, which amounts to 40% of spread produced by the two ensemble configurations that use tropospheric perturbations. Nevertheless, the difference between the S-SV and ST-SV ensembles is smaller than one would expect from the associated singular values. One of the reasons may be that stochastic physics interferes with the SV properties. To that end we also ran two ensemble configurations with perturbations solely based on ST-SV's or S-SV's, but without stochastic physics. Switching off stochastic physics in the S-SV and ST-SV only ensembles reduces the spread and shows a clear distinction in case of Z500 depending on whether ST-SV or S-SV perturbations are used, see Fig. 8. The Z50 results again reveal the reduced growth of the S-SV perturbations after the optimization time.
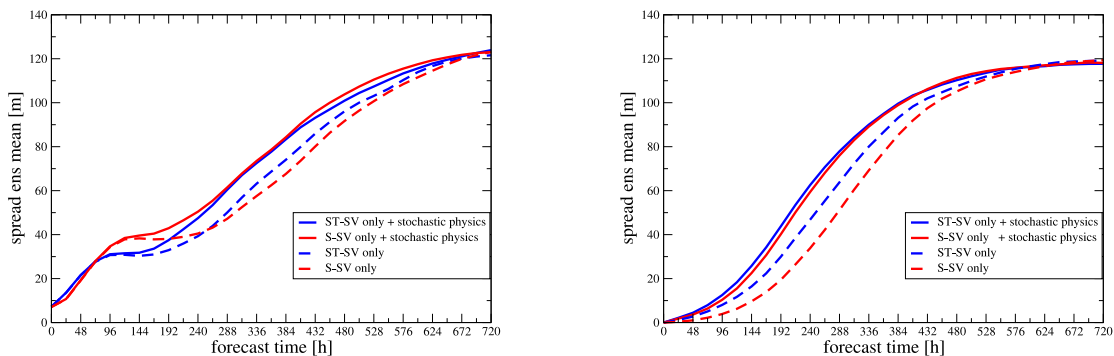
Figure 8: Left panel: Z50 standard deviation for ensembles using only S-SV's (red) or ST-SV's (blue) perturbations. Ensembles with stochastic physics (not) active are given by solid (dashed) lines; Right panel: same but for Z500.
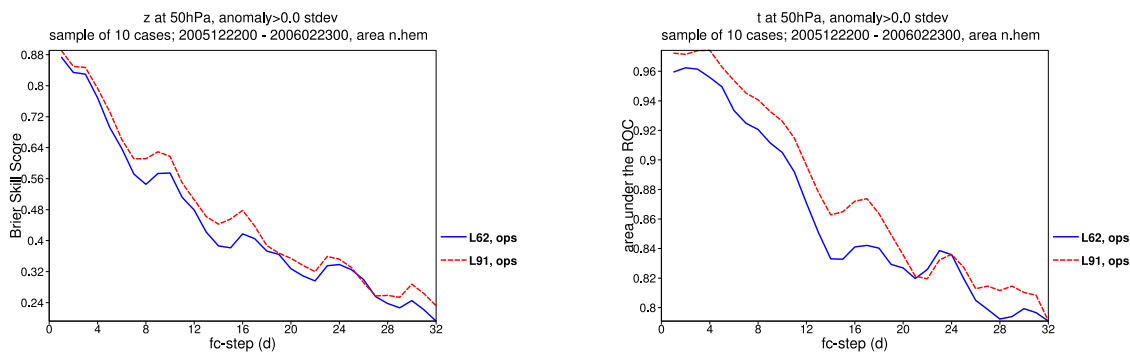

Figure 9: Probability scores for L62 (solid blue) and L91 (dashed red) ensembles with operational setting.
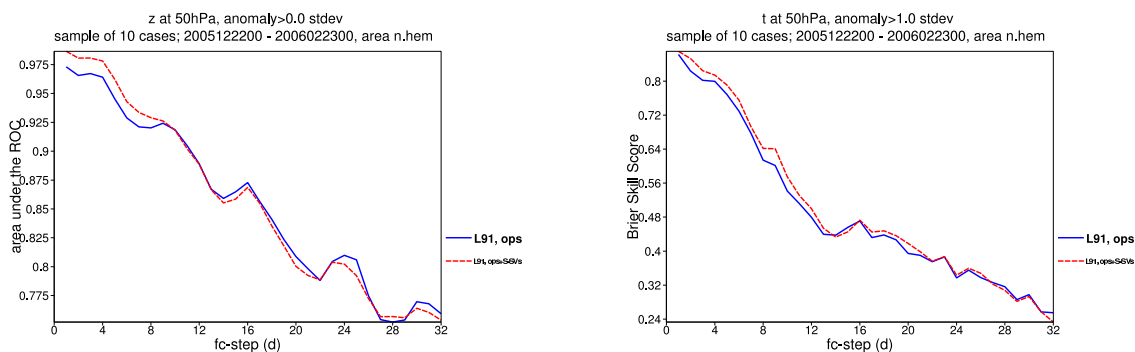

Figure 10: Probability scores for L91 ensembles with operational setting (solid blue) and with S-SV's added (dashed red).

4.3   Probability scores

Increasing the vertical resolution from 62 to 91 levels has a positive impact on the probability scores mainly in the stratosphere. See Fig. 9 for temperature and geopotential height at 50 hPa (other thresholds give similar results). For the troposphere the impact is neutral. Extending L62 and L91 ensembles with operational setting from 10 to 25 cases gave similar results. Using stratospheric perturbations in an ensemble configuration again improves the probability scores in the stratosphere, see Fig. 10. The impact on the tropospheric scores is neutral, apart from the polar region, where scores improve (not shown).

5   Conclusions

– Adjoint techniques are useful in identifying structures that may play a role in the stratosphere-troposphere interaction.
– Increasing vertical resolution (i.e., L62 vs. L91) improves ensemble performance, most notably in the stratosphere.
– Stratospheric perturbations are capable to produce substantial spread in the stratosphere as well as in the troposphere.
– Stratospheric perturbations improve ensemble performance in the stratosphere and have neutral impact on tropospheric probability scores (apart from improved performance in the polar region).
– Combining stratospheric and tropospheric perturbations does not simply lead to more ensemble spread in the troposphere.

6   References

Baldwin, M. P., J. Dunkerton, 1999: Propagation of the Arctic Oscillation from the stratosphere to the troposphere. J. Geophys. Res. **104**, 30937–30946.

Baldwin, M.P., D.B. Stephenson, D.W.J. Thompson, T.J. Dunkerton, A.J. Charlton, A. O'Neill, 2003: Stratospheric memory and skill of extended-range weather forecasts. Science. **301**, 636–640.

Boville, B.A., 1984: The influence of the polar night jet on the tropospheric circulation in a GCM. Science. **41**, 1132–1142.

Buizza, R., T.N. Palmer, 1995: The singular vector structure of the atmospheric global circulation. J. Atmos. Sci. **52**, 1434–1456.

Charlton, A.J., A. O'Neill, D.B. Stephanson, W.A. Lahoz, M.P. Baldwin, 2003: Can knowledge of the state of the stratosphere be used to improve statistical forecasts of the troposphere. Quart. J. Roy. Meteor. Soc. **129**, 3205–3224.

Charney, J.G., P.G. Drazin, 1961: Propagation of planetary-scale disturbances form the lower into the upper atmosphere. J. Geophys. Res., **66**, 83-109.

Christiansen, B., 2005: Downward propagation and statistical forecast of the near-surface weather. J. Geophys. Res. **110**, D14104.

Errico, R.M., 2000: Interpretations of the total energy and rotational energy applied to determination of singular vectors. Quart. J. Roy. Meteor. Soc. **126A**, 1581–1599.

Hartmann, D. L., T.N. Palmer, R. Buizza, 1996: Finite-time instabilities of lower-stratospheric flow. J. Atmos. Sci. **53**, 2130–2143.

Haynes, P, 2005: Stratosphere dynamics. Ann. Rev. Fluid. Mech. **37**, 263–293.

Hooghoudt, J.-O., J. Barkmeijer, 2007: The interaction between the stratosphere and the troposphere as revealed by singular vectors. Meteorol. Z. **16**, 723-739.

Jung, T., J. Barkmeijer, 2006: Sensitivity of the tropospheric circulation to changes in the strength of the stratospheric polar vortex. Mon. Wea. Rev. **134**, 2191–2207.

Jung, T., M. Leutbecher, 2007: Performance of the ECMWF forecasting sytem in the Artic during winter. Quart. J. Roy.Meteor. Soc. **133**, 1327–1340.

Labitzke, K., 1999: The Stratosphere: Phenomena, History, and Relevance. Springer: 179 pages.

Siegmund, P., 2005: Stratospheric polar cap mean height and temperature as extended-range weather predictors. Mon. Wea. Rev. **133**, 2436–2448.

Vitart, F., 2004: Monthly forecasting at ECMWF. Mon. Wea. Rev. **132**, 2761–2779.